

Tuning Magnetism in Ising-type van der Waals Magnet FePS_3 by Lithium Intercalation

Dinesh Upreti¹, Rabindra Basnet^{1,2}, M M Sharma¹, Santosh Karki Chhetri¹, Gokul Acharya¹, Md Rafique Un Nabi^{1,3}, Josh Sakon⁴, Bo Da⁵, Mansour Mortazavi³, Jin Hu^{1,3*}

¹Department of Physics, University of Arkansas, Fayetteville, AR 72701, USA

²Department of Chemistry & Physics, University of Arkansas at Pine Bluff, Pine Bluff, Arkansas 71603, USA

³MonArk NSF Quantum Foundry, University of Arkansas, Fayetteville, Arkansas 72701, USA

⁴Department of Chemistry & Biochemistry, University of Arkansas, Fayetteville, AR 72701, USA

⁵Center for Basic Research on Materials, National Institute for Materials Science, Tsukuba, Ibaraki 305-0044, Japan

Abstract

Recently, layered materials transition metal thiophosphate MPX_3 (M = transition metals, X = S or Se) have gained significant attention because of their rich magnetic, optical, and electronic properties. Specifically, the diverse magnetic structures and the robustness of magnetism in the two-dimensional limit have made them prominent candidates to study two-dimensional magnetism. Numerous efforts such as substitutions and interlayer intercalations have been made to tune the properties of these materials, which has greatly deepened the understanding of the underlying mechanisms that govern the properties. In this work, we focus on modifying the

magnetism of Ising-type antiferromagnet FePS₃ using electrochemical lithium intercalation. Our work unveils the effectiveness of electrochemical intercalation as a controllable tool to modulating magnetism, including tuning magnetic ordering temperature and inducing low temperature spin-glass state, offering an approach for implementing this material into applications.

*jinhu@uark.edu

I. Introduction

Emerging magnetism in van der Waals (vdWs) magnets provides a deeper understanding of phenomena arising from two-dimensional (2D) magnetism such as magnetic skyrmions[1,2] and other spin textures[3], which shed light on future spintronic applications[4–7]. This has attracted significant efforts to effectively manipulate magnetic ordering and spin orientations in vdW magnetic materials, such as chemical substitution [8–10], high-pressure [11–14], and strain effect [15]. The magnetic vdW-type transition metal thiophosphate MPX_3 (M = transition metals, X = S or Se) is a large antiferromagnetic (AFM) material family, in which each transition metal M carries localized moments in a honeycomb lattice and sandwiched by chalcogen X atom layers[16–19]. MPX_3 compounds exhibit AFM ground states in bulk form. Such long-range magnetic orders persist even in the two-dimensional (2D) limit for certain MPX_3 such as FePS₃ and MnPS₃ [20–22]. The magnetic properties of MPX_3 are strongly dependent on the choice of M and X , which has motivated extensive metal M [23–32] and chalcogen X [8,33,34] substitution studies to tune magnetism. In addition, one effective route to tune magnetic properties in vdW materials is inter-layer intercalation of guest ions, atoms, or molecules[35–45]. The layered structure of MPX_3 compounds allows for inter-layer intercalation of guest species such as pyridine, lithium (Li), and

ammonia which has also been demonstrated as an efficient approach to tune magnetism in MnPS_3 , NiPS_3 , and FePS_3 [36–38,40,42–44]. These intercalation studies have revealed signatures of ferrimagnetism[37,40], weak ferromagnetism[36], and spin glass[38], as well as the modulation of magnetic ordering temperatures[36,42–44].

Among various MPX_3 compounds, FePS_3 displays Ising-type magnetism that is characterized by out-of-plane magnetic moments[46]. The Ising-type magnetism in FePS_3 has been proposed to stem from large crystal electric field arising from the strong trigonal distortion of the FeS_6 octahedra[47,48]. Because of the strong magnetic anisotropy associated with the Ising-type magnetism, the long-range magnetic order in FePS_3 persists down to the single-layer[20]. However, given the zero net magnetization of the AFM ground state, the magnetic characterization in atomically thin layers is challenging. So far, the persistence of the 2D AFM order of FePS_3 has been probed using Raman spectroscopy which is an indirect probe[20]. This has hindered the potential application of FePS_3 though it is one of the first known 2D magnets. Establishing a ferromagnetic (FM) order in FePS_3 would make the study of 2D magnetism more accessible and convenient by direct magnetic characterization tools such as Kerr rotation [5,49] and magnetic force microscope[50]. Unfortunately, magnetism in FePS_3 is rather robust against common tuning approaches such as chemical substitution in either metal or chalcogen sites[33]. Earlier theoretical studies[51,52] have predicted that charge doping may induce a FM order in MPX_3 . Hence, compared to isovalent substitutions, inter-layer intercalation that usually results in charge doping might be an effective strategy to induce ferromagnetism in MPX_3 . Previous intercalation studies on FePS_3 using molecular intercalants have revealed a possible spin-glass state[38] and a reduction in magnetic ordering temperature [43]. In addition, lithium is another good intercalant because of its smaller atomic size which may allow for a greater amount of intercalant without strong structure

modifications. Li intercalation on FePS₃ has been studied a few decades ago but both unchanged [53] and suppressed[44] transition temperature have been reported, which motivates us to revisit the effect of Li intercalation on magnetism in FePS₃.

In this study, we performed systematic electrochemical intercalation of lithium in FePS₃ and studied the evolution of magnetic properties. From the magnetic susceptibility measurements, the AFM transition temperature is found to reduce for heavily intercalated samples. In addition, the zero-field cooling (ZFC) and field cooling (FC) susceptibility exhibit substantial irreversibility and magnetic hysteresis near zero magnetic fields at low temperatures, which are likely attributed to weak ferromagnetism due to spin-glass state or vacancy-induced magnetism. Such engineering of magnetism in FePS₃ offers a promising platform to tune Ising-type anisotropy that could be extended to other Ising-type magnetic systems.

II. Experiment

Single crystals of FePS₃ were synthesized using a chemical vapor transport method with I₂ as the transport agent. The stoichiometric mixture of Fe, P, and S powder was vacuum-sealed in a quartz tube and placed in a two-zone furnace with a temperature gradient from 750⁰-650⁰C for one week. The electrochemical intercalations of Li into FePS₃ single crystal were performed in an electrochemical workstation (Battery testing system 8.0, Neware) in a similar way reported previously[37]. The elemental composition and crystal structure of the obtained FePS₃ crystals were determined by energy dispersive x-ray spectroscopy (EDXS) and x-ray diffraction (XRD), respectively. The magnetic properties were measured using a Magnetic Property Measurement System (MPMS3, Quantum Design).

Different techniques such as liquid/wet chemical intercalation[36,38,39,54,55], gaseous intercalation[56,57], and electrochemical intercalation[37,53,58] has been adopted to intercalate layered compounds to tune their properties. The liquid chemical process is carried out by immersing the host in a guest solution. However, this process is easily accompanied by the exfoliation of the bulk materials to layers which hinders the further applications[59]. Additionally, the degree of intercalation is not easily controllable. Gaseous intercalations are performed by a vapor transport technique[56,57] in which the host material and guest intercalant are placed separately at cold and hot zones respectively in a two-zone furnace. The gaseous form of the intercalant is transferred to the cold zone and intercalates into the host material. While this method has several benefits such as scalability and a higher degree of intercalation, it is irreversible which inhibits the potential application in batteries, sensors, and optical switches[59]. Compared to the above methods, electrochemical intercalation is a controllable approach[59,60] for which the amount of intercalant can be controlled by the applied electrical current and the duration of intercalation[37]. Moreover, the intercalation is reversible, making it suitable for devices and energy storage applications[59].

Figures 1(a) and 1(b) show the schematic of the electrochemical intercalation of Li in the vdW gap of FePS₃ single crystals. In this setup, the FePS₃ single crystals and Li-chips act as anode and cathode, respectively, where both electrodes were dipped in an electrolytic solution of Li bis-trifluoro methane sulfonamide salt in dimethoxy-ethane and dioxolane mixed in the ratio of 1:1. The intercalation was performed using a coin battery setup as reported previously[37], and the batteries were prepared inside an argon-filled glovebox. Electrochemical intercalation was carried out with a constant discharge current of 20 μ A similar to the previous Li-intercalation study on NiPS₃[37]. To promote homogeneous intercalation, the experiments were performed at 50° C. The

amount of Li intercalation was controlled by varying the intercalation time. FePS₃ single crystals with similar mass were chosen to ensure controllable study. Because of the difficulty of probing Li using the common x-ray-based techniques such as XRD and EDS, it is not possible to accurately determine the content of the intercalated Li. Instead, we label the samples as sample #1 (pristine FePS₃), #2, #3, #4, and #5, in which the Li amount systematically increases according to the duration of the electrochemical intercalation process and lattice constant, as will be shown below.

III. Result and Discussion

The images of the sample #1 to #4 are shown in Fig. 1(c). Compared with the pristine sample, crystals somewhat lose metal luster upon increasing intercalation time. For sample #5 with the longest electrochemical intercalation and hence the highest amount of Li, it became powder-like and we did not include it in comparison. A similar trend was observed for Li intercalated NiPS₃[37]. The crystal structures of the intercalated samples were characterized by powder x-ray diffraction (PXRD). As shown in Figure 1c, sample #2 and #3 display highly similar diffraction patterns as the pristine sample (sample #1) except for some tiny peak shift, indicating that the crystal structure of FePS₃ is maintained up on Li intercalation. For sample #4, main diffraction peaks are broadened but still match with that of the pristine sample. The emergence of additional diffraction peaks as indicated by asterisks is likely due to the formation of Li₃PS₄ or Li₄P₂S₆ on the edge of the sample[37,61]. The intercalated Li atoms are expected to occupy the vdW gap, but the exact location cannot be identified by common X-ray-based techniques. Nevertheless, the evolution of crystal lattice with intercalation provides clear evidence for successfully intercalation. As shown in Fig. 1c, Rietveld structure refinement reveals an unchanged space group of *C2/m* up

to sample #4. For sample #5, the refinement can only yield lattice parameters without reliable atomic positions. Therefore, in this work, we limit the studies to sample #1 to #4. Table 1 summarizes the refined lattice parameters. Overall, the in-plane lattice parameters a and b show subtle variations up on Li intercalation, which has also been observed in the pyridine-intercalated MnPS_3 [36]. In contrast, the out-of-plane lattice parameter c shows minor changes for samples #2 and #3 but increases strongly by 0.83% for sample #4 and 9.7% for #5. The above observations clearly reveal the control of Li amount by the duration of electrochemical intercalation, and suggest that the doped Li most likely intercalates into the vdW gap, as illustrated in Fig. 1b.

Previous studies have revealed that intercalation on MPX_3 successfully tunes magnetic properties including the emergence of ferrimagnetism[37,40], ferromagnetism[36], and spin glass[38], as well as the tuning of ordering temperature [36,42,43]. To study the effects of Li intercalation on FePS_3 , the temperature and field dependences of magnetization were examined. The pristine FePS_3 is characterized by Ising-type antiferromagnetism with out-of-plane moment orientation below 120 K [47,62]. The Ising-type magnetism in FePS_3 is manifest by substantial anisotropy even in the paramagnetic (PM) state, with the out-of-plane magnetic susceptibility χ_{\perp} (measured with an out-of-plane magnetic field $H \perp ab$) much larger than the in-plane one χ_{\parallel} (measured with an in-plane magnetic field $H \parallel ab$)[47]. As shown in Fig. 2, the strong anisotropy with much greater χ_{\perp} in the PM state is also observed in our Li-intercalated FePS_3 samples, implying robust Ising-type magnetism against intercalation in FePS_3 . Compared to the higher temperature PM state, the low-temperature AFM state is more significantly affected by Li intercalation. The pristine FePS_3 displays nearly temperature-independent susceptibility in the AFM state (Fig. 2a), whereas strong low-temperature susceptibility upturns emerge in Li-intercalated samples (Figs. 2b-2d). Furthermore, unlike the perfectly overlapped ZFC and FC

susceptibility in FePS₃, Li-intercalated samples display clear irreversibility at low temperatures, as indicated by T_{irr} (black triangles) in Figs. 2b-2d. These observations suggest a possible spin-glass state or vacancy-induced ferromagnetism up on Li intercalation, as will be discussed later.

In addition to the modification to the low-temperature susceptibility, Li intercalation also tunes the AFM ordering temperature T_{N} in FePS₃. As shown in Fig. 2a, at the temperature that magnetic susceptibility reaches maximum ($T_{\text{max}} \approx 130\text{K}$, dashed lines), FePS₃ displays a broad susceptibility hump instead of a sharp transition. AFM transition characterized by sharp susceptibility drop occurs at lower temperature of 120 K (pink dotted lines). This susceptibility hump above T_{N} has also been seen in previous studies on FePS₃ and many other MPX_3 compounds and has been attributed to the in-plane short-range magnetic correlations of the layered MPX_3 [47]. Increasing the Li content from sample #2 to sample #4 reduces both T_{max} and T_{N} , as shown in Figs 2c-2d. The susceptibility hump above T_{N} is gradually suppressed and the temperature difference between T_{max} and T_{N} is reduced. The observed evolution of T_{max} and T_{N} with Li intercalation is summarized in Fig. 3. Because of the difficulty in determining the exact content of Li as stated above, here we use the interlayer spacing d which measures the vdW gap to characterize the degree of Li intercalation, because intercalating Li elongates d as revealed by XRD discussed above. As shown in Fig. 3, systematic suppression of T_{N} with intercalation from 120 K in the pristine FePS₃ to 91 K in sample #4 is seen, which is accompanied by an elongation of d by 0.8%. Our direct observation of suppression of T_{N} in FePS₃ by intercalation is consistent with the previous report in which magnetic transition is determined by Raman scattering[44]. Moreover, unlike the need for more than 50% increase in d to suppress T_{N} by 35%[43], in this work 24% T_{N} reduction is realized by less than 1% change in d .

To obtain some insights into the correlation between interlayer distance and T_N , in Table 2 we summarize the relative changes of interlayer distance and T_N normalized to that of the pristine samples for FePS₃[38,43], together with MnPS₃ [36,40] and NiPS₃[37,43] which have been relatively intensively studied by intercalation. Both Li- and organic-ion-intercalations are included in the table, which facilitates comparison of a wide range of changes in d . Interestingly, magnetic ordering temperature in FePS₃ and MnPS₃ can be suppressed by intercalation, but it is much more robust in NiPS₃ against 55% increase in d . Such a difference might be associated with the different mechanisms for magnetism in those materials. For example, it has been reported that, because magnetism is governed by direct exchange in MnPS₃ but superexchange in NiPS₃, T_N is only slightly suppressed in MnPS₃ but strongly enhanced in NiPS₃ by Se substitution[24]. For the intercalation study, considering the unchanged insulating nature and the accompanied d enhancement, the observations summarized in Table 2 suggest that the interlayer magnetic exchange J_z might play a non-trivial role in governing magnetism in FePS₃ and MnPS₃, which is generally overlooked since magnetism in MPX_3 family has been generally considered to be mainly governed by the intralayer exchange interactions [62,63]. Indeed, recent studies suggest that interlayer exchange interaction may not be negligible in MPX_3 [64,65]. Nevertheless, this appears conflict to the experimental observation of the very robust AFM long-range order with unchanged T_N in the FePS₃ monolayer[20].

In addition to the role of interlayer interaction, other mechanisms might also give rise to reduced T_N . An early Raman study on Li-intercalated FePS₃[44] has attributed the T_N reduction to the suppression of in-plane exchange interactions caused by magnetic fluctuations from a random distribution of lithium. In addition, the lowering of magnetic ordering temperature is also observed in the pyridine-intercalated MnPS₃[36], which has been ascribed to magnetic dilution due to the

vacancies. Though PXRD is unable to reveal vacancies, their presence might be supported by our magnetic susceptibility measurements. As stated above, FePS₃ displays a broad hump at susceptibility maxima above T_N similar to many other MPX_3 compounds (Fig. 2). The temperature T_{\max} for such hump is relatively more efficiently suppressed and eventually disappears (i.e., merge with T_N) by Li intercalation. Since such susceptibility hump is believed to be caused by the in-plane short-range magnetic correlation above T_N [47], its suppression can be attributed to the suppression of in-plane exchange. Furthermore, the T_N reduction may also be associated with carrier doping which has been observed in heavily doped europium chalcogenides[66]. However, this is inconsistent with the fact that the Li-intercalated FePS₃ samples remain highly insulating. To elucidate the actual mechanism for T_N suppression, additional theoretical and experimental effort is needed.

In addition to the diminution of magnetic ordering temperature, a bifurcation between ZFC and FC susceptibility has been observed at a temperature below T_N , at around 20 K for samples #2 and #3, and 66 K for sample #4, as denoted by T_{irr} in Fig 2 and summarized in Fig. 3. Such irreversibility implies the rise of the FM interactions at low temperatures, which is further supported by the field dependence of magnetization. As shown in Fig. 3, up on Li intercalation, magnetic hysteresis loop gradually develops in out-of-plane magnetization (measured with $H \perp ab$) at $T = 2$ K but is negligible in in-plane magnetization (measured with $H // ab$). Both out-of-plane and in-plane magnetizations lack saturation behavior up to 7 T, suggesting that the ferromagnetic correlations, if exist, may not develop into a long-range order. Such ferromagnetic correlations might be caused by magnetic impurities, vacancy magnetism, or moment canting. The presence of magnetic impurities is less likely because no such impurities have been probed by XRD as described above. Vacancies in the metal sites may occur, which has also been proposed in the 4-

aminopyridine intercalated FePS₃[45]. In addition, vacancies may also give rise to moment canting. Careful crystal structure and magnetic structure studies are needed to clarify such a scenario.

In addition to ferromagnetic correlations, the development of a spin glass state also explains the observed irreversibility. Spin glass can arise with strong geometric or magnetic frustrations. Given the comparable FM nearest-neighbor interaction J_1 and AFM third nearest-neighbor interaction J_3 in FePS₃[46], the magnetic frustration arising from competing FM J_1 and AFM J_3 is possible when intercalated Li disturbs the exchange interactions. Indeed, spin glass states upon intercalation in A[NH₃]_xFePS₃ (A = Li, K) [38] and metal substitution in Mn_{1-x}Fe_xPS₃[32] have been reported. Interestingly, magnetic irreversibility has not been observed in Li-intercalated NiPS₃[37], which can be understood in terms of the lack of strongly competing magnetic exchange interactions since the magnetism in NiPS₃ is dominated by the much stronger AFM J_3 interaction[63].

IV. Conclusion

In conclusion, we have successfully intercalated lithium in the FePS₃ single crystals using an electrochemical approach. The Ising type magnetism in the pristine FePS₃ is found to be robust towards lithium intercalation, while a suppression of T_N occurs with high amount of Li amount. The reduction in T_N suggests that the interlayer interactions may play a role in stabilizing magnetic ordering temperature in some MPX_3 compounds. In addition to the decrease in T_N , magnetic irreversibility below T_N is seen along with the magnetic hysteresis, which might be attributed to a spin glass state arising from the magnetic frustrations caused by intercalation. The successful

tuning of magnetic ordering temperature and spin glass state with Ising-type magnetism intact in FePS₃ offers an alternative and efficient path in modulating magnetism of 2D materials. The controllable electrochemical intercalation and its easy integration in devices further provides an approach for implementing this material in applications.

Acknowledgments

This work was primarily (crystal growth and intercalation) supported by the U.S. Department of Energy, Office of Science, Basic Energy Sciences program under Grant No. DE-SC0022006. M.R.U.N acknowledges the MonArk NSF Quantum Foundry, which is supported by the National Science Foundation Q-AMASE-i program under NSF award No. DMR-1906383. R.B, M.M.S, and M.M acknowledges μ -ATOMS, an Energy Frontier Research Center funded by DOE, Office of Science, Basic Energy Sciences, under Award No. DE-SC0023412 (Refinement and part of the magnetic property analysis). J. S. acknowledges the support from NIH under award P20GM103429 for the powder XRD experiment.

References

- [1] Ding B, Li Z, Xu G, Li H, Hou Z, Liu E, Xi X, Xu F, Yao Y and Wang W 2019 Observation of Magnetic Skyrmion Bubbles in a van der Waals Ferromagnet Fe_3GeTe_2 *Nano Lett* **20** 868-873
- [2] Tong Q, Liu F, Xiao J and Yao W 2018 Skyrmions in the Moiré of van der Waals 2D Magnets *Nano Lett* **18** 7194-7199
- [3] Du K, Huang F-T, Kim J, Lim S J, Gamage K, Yang J, Mostovoy M, Garlow J, Han M-G, Zhu Y and Cheong S-W 2021 Topological spin/structure couplings in layered chiral magnet $\text{Cr}_1/3\text{TaS}_2$: The discovery of spiral magnetic superstructure *Proc. Natl. Acad. Sci.* **118** e2023337118
- [4] Cai X, Song T, Wilson P N, Clark G, He M, Zhang Z, Taniguchi T, Watanabe K, Yao W, Xiao D, McGuire A M, Cobden H D and Xu X 2019 Atomically Thin CrCl_3 : An In-Plane Layered Antiferromagnetic Insulator *Nano Lett* **19** 3993-3998
- [5] Huang B, Clark G, Navarro-Moratalla E, Klein D R, Cheng R, Seyler K L, Zhong D, Schmidgall E, McGuire M A and Cobden D H 2017 Layer-dependent ferromagnetism in a van der Waals crystal down to the monolayer limit *Nature* **546** 270–3
- [6] Sierra J F, Fabian J, Kawakami R K, Roche S and Valenzuela S O 2021 Van der Waals heterostructures for spintronics and opto-spintronics *Nat. Nanotechnol.* **16** 856–68

- [7] Klein R D, MacNeill D, Lado L J, Soriano D, Navarro-Moratalla E, Watanabe K, Taniguchi T, Manni S, Canfield P, Fernandez-Rossier J and Jarillo-Herrero P 2018 Probing magnetism in 2D van der Waals crystalline insulators via electron tunneling *Science* **360** 1218-1222
- [8] Han H, Lin H, Gan W, Liu Y, Xiao R, Zhang L, Li Y, Zhang C and Li H 2023 Emergent mixed antiferromagnetic state in $\text{MnPS}_3_{(1-x)}\text{Se}_3_x$ *Appl. Phys. Lett.* **122** 033101
- [9] May A F, Du M-H, Cooper V R and McGuire M A 2020 Tuning magnetic order in the van der Waals metal Fe_5GeTe_2 by cobalt substitution *Phys. Rev. Mater.* **4** 074008
- [10] Abramchuk M, Jaszewski S, Metz K R, Osterhoudt G B, Wang Y, Burch K S and Tafti F 2018 Controlling Magnetic and Optical Properties of the van der Waals Crystal $\text{CrCl}_{3-x}\text{Br}_x$ via Mixed Halide Chemistry *Adv. Mater.* **30** 1801325
- [11] Song T, Fei Z, Yankowitz M, Lin Z, Jiang Q, Hwangbo K, Zhang Q, Sun B, Taniguchi T, Watanabe K, McGuire M A, Graf D, Cao T, Chu J-H, Cobden D H, Dean C R, Xiao D and Xu X 2019 Switching 2D magnetic states via pressure tuning of layer stacking *Nat. Mater.* **18** 1298–302
- [12] Wang Y, Ying J, Zhou Z, Sun J, Wen T, Zhou Y, Li N, Zhang Q, Han F, Xiao Y, Chow P, Yang W, Struzhkin V V, Zhao Y and Mao H 2018 Emergent superconductivity in an iron-based honeycomb lattice initiated by pressure-driven spin-crossover *Nat. Commun.* **9** 1914
- [13] Wang Y, Zhou Z, Wen T, Zhou Y, Li N, Han F, Xiao Y, Chow P, Sun J, Pravica M, Cornelius L A, Yang W and Zhao Y 2016 Pressure-Driven Cooperative Spin-Crossover, Large-Volume Collapse, and Semiconductor-to-Metal Transition in Manganese (II) Honeycomb Lattices *J. Am. Chem. Soc.* **138** 15751-15757

- [14] Coak M J, Son S, Daisenberger D, Hamidov H, Haines C R S, Alireza P L, Wildes A R, Liu C, Saxena S S and Park J-G 2019 Isostructural Mott transition in 2D honeycomb antiferromagnet $V_{0.9}PS_3$ *Npj Quantum Mater.* **4** 1–6
- [15] Wang Y, Wang C, Liang S-J, Ma Z, Xu K, Liu X, Zhang L, Admasu A S, Cheong S-W, Wang L, Chen M, Liu Z, Cheng B, Ji W and Miao F 2020 Strain-Sensitive Magnetization Reversal of a van der Waals Magnet *Adv. Mater.* **32** 2004533
- [16] Ouvrard G, Brec R and Rouxel J 1985 Structural determination of some MPS_3 layered phases (M = Mn, Fe, Co, Ni and Cd) *Mater. Res. Bull.* **20** 1181–9
- [17] Klungen W, Eulenberger G and Hahn H 1973 Über die Kristallstrukturen von $Fe_2P_2Se_6$ und $Fe_2P_2S_6$ *Z. Für Anorg. Allg. Chem.* **401** 97–112
- [18] Wang F, Shifa A T, Yu P, He P, Liu Y, Wang F, Wang Z, Zhan X, Lou X, Xia F and He J 2018 New Frontiers on van der Waals Layered Metal Phosphorous Trichalcogenides Advanced Functional Materials *Adv. Funct. Mater.* **28** 1802151
- [19] Du K, Wang X, Liu Y, Hu P, Utama M I B, Gan C K, Xiong Q and Kloc C 2016 Weak Van der Waals Stacking, Wide-Range Band Gap, and Raman Study on Ultrathin Layers of Metal Phosphorus Trichalcogenides *ACS Nano* **10** 1738–43
- [20] Lee J-U, Lee S, Ryoo J H, Kang S, Kim T Y, Kim P, Park C-H, Park J-G and Cheong H 2016 Ising-Type Magnetic Ordering in Atomically Thin $FePS_3$ *Nano Lett.* **16** 7433–8

- [21] Long G, Henck H, Gibertini M, Dumcenco D, Wang Z, Taniguchi T, Watanabe K, Giannini E and Morpurgo A F 2020 Persistence of Magnetism in Atomically Thin MnPS₃ Crystals *Nano Lett.* **20** 2452–9
- [22] Kim K, Lim S Y, Kim J, Lee J-U, Lee S, Kim P, Park K, Son S, Park C-H, Park J-G and Cheong H 2019 Antiferromagnetic ordering in van der Waals 2D magnetic material MnPS₃ probed by Raman spectroscopy *2D Mater.* **6** 041001
- [23] Chandrasekharan N and Vasudevan S 1996 Dilution of a layered antiferromagnet: Magnetism in Mn_xZn_{1-x}PS₃ *Phys. Rev. B* **54** 14903–6
- [24] Basnet R, Wegner A, Pandey K, Storment S and Hu J 2021 Highly sensitive spin-flop transition in antiferromagnetic van der Waals material MPS₃ (M=Ni} and Mn) *Phys. Rev. Mater.* **5** 064413
- [25] Shemerliuk Y, Zhou Y, Yang Z, Cao G, Wolter A U, Büchner B and Aswartham S 2021 Tuning magnetic and transport properties in quasi-2D (Mn_{1-x}Ni_x) 2P2S6 single crystals *Electron. Mater.* **2** 284–98
- [26] Bhutani A, Zuo J L, McAuliffe R D, Dela Cruz C R and Shoemaker D P 2020 Strong anisotropy in the mixed antiferromagnetic system Mn_{1-x}Fe_xPSe₃ *Phys. Rev. Mater.* **4** 034411
- [27] Goossens D J and Hicks T J 1998 The magnetic phase diagram of *J. Phys. Condens. Matter* **10** 7643
- [28] Goossens D J, Brazier-Hollins S, James D R, Hutchison W D and Hester J R 2013 Magnetic structure and glassiness in Fe_{0.5}Ni_{0.5}PS₃ *J. Magn. Magn. Mater.* **334** 82–6

- [29] Manríquez V, Barahona P and Peña O 2000 Physical properties of the cation-mixed M' MPS₃ phases *Mater. Res. Bull.* **35** 1889–95
- [30] Lee S, Park J, Choi Y, Raju K, Chen W-T, Sankar R and Choi K-Y 2021 Chemical tuning of magnetic anisotropy and correlations in Ni_{1-x}Fe_xPS₃ *Phys. Rev. B* **104** 174412
- [31] Basnet R, Upreti D, Patel T, Chhetri S K, Acharya G, Nabi M R U, Sharma M M, Sakon J, Mortazavi M and Hu J 2024 Field-induced spin polarization in lightly Cr-substituted layered antiferromagnet NiPS₃
- [32] Masubuchi T, Hoya H, Watanabe T, Takahashi Y, Ban S, Ohkubo N, Takase K and Takano Y 2008 Phase diagram, magnetic properties and specific heat of Mn_{1-x}Fe_xPS₃ *J. Alloys Compd.* **460** 668–74
- [33] Basnet R, Patel T, Wang J, Upreti D, Chhetri S K, Acharya G, Nabi M R U, Sakon J and Hu J 2024 Understanding and Tuning Magnetism in Layered Ising-Type Antiferromagnet FePSe₃ for Potential 2D Magnet *Adv. Electron. Mater.* 2300738
- [34] Basnet R, Kotur K M, Rybak M, Stephenson C, Bishop S, Autieri C, Birowska M and Hu J 2022 Controlling magnetic exchange and anisotropy by nonmagnetic ligand substitution in layered MPX₃ (M=Ni, Mn; X= (S, Se) *Phys. Rev. Res.* **4** 023256
- [35] Huang X, Xu J, Zeng R, Jiang Q, Nie X, Chen C, Jiang X and Liu J-M 2021 Li-ion intercalation enhanced ferromagnetism in van der Waals Fe₃GeTe₂ bilayer *Appl. Phys. Lett.* **119** 012405

- [36] Joy P A and Vasudevan S 1992 The intercalation reaction of pyridine with manganese thiophosphate, MnPS_3 *J. Am. Chem. Soc.* **114** 7792–801
- [37] Basnet R, Ford D, TenBarge K, Lochala J and Hu J 2022 Emergence of ferrimagnetism in Li-intercalated NiPS_3 *J. Phys. Condens. Matter* **34** 434002
- [38] Feng X, Guo Z, Yan X, Deng J, Wu D, Zhang Z, Sun F and Yuan W 2021 $\text{A}(\text{NH}_3)_x \text{FePS}_3$ (A = Li, K): intercalated Fe thiophosphate via the liquid ammonia method *Mater. Chem. Front.* **5** 2715–23
- [39] Yang C, Chen X, Qin J, Yakushi K, Nakazawa Y and Ichimura K 2000 Synthesis, Characterization, and Magnetic Properties of Intercalation Compound of 1,10-Phenanthroline with Layered MnPS_3 *J. Solid State Chem.* **150** 281–5
- [40] Zhou H, Su X, Zhang X, Chen X, Yang C, Qin J and Inokuchi M 2006 Intercalation of amino acids into layered MnPS_3 : Synthesis, characterization and magnetic properties *Mater. Res. Bull.* **41** 2161–7
- [41] Xie S L, Husremovic S, Gonzalez O, Craig M I and Bediako K D 2018 Structure and Magnetism of Iron- and Chromium-Intercalated Niobium and Tantalum Disulfides *J. Am. Chem. Soc.* **144** 9525-9542
- [42] Clement R, Garnier O and Mathey Y 1982 INTERCALATION-INDUCED MODIFICATIONS OF THE OPTICAL AND MAGNETIC PROPERTIES OF FePS_3 AND NiPS_3 LAYER PHASES

- [43] Li C, Hu Z, Hou X, Xu S, Wu Z, Du K, Li S, Xu X, Chen Y, Wang Z, Mu T, Xia T-L, Guo Y, Normand B, Yu W and Cui Y 2024 Molecular intercalation in the van der Waals antiferromagnets FePS₃ and NiPS₃ *Phys. Rev. B* **109** 184407
- [44] Senkine T, Jouanne M, Julien C and Balkanski M 1989 Raman scattering in the antiferromagnet FePS₃ intercalated with lithium *Mater. Sci. Eng. B* **3** 91–5
- [45] Chen X, Zou L, Zhang X, Qin J, Inokuchi M and Kinoshita M 2003 The Intercalation of 4-Aminopyridine into Layered FePS₃ *J. Incl. Phenom. Macrocycl. Chem.* **46** 105–10
- [46] Lançon D, Walker H C, Ressouche E, Ouladdiaf B, Rule K C, McIntyre G J, Hicks T J, Rønnow H M and Wildes A R 2016 Magnetic structure and magnon dynamics of the quasi-two-dimensional antiferromagnet FePS₃ *Phys. Rev. B* **94** 214407
- [47] Joy P A and Vasudevan S 1992 Magnetism in the layered transition-metal thiophosphates MPS₃ (M=Mn, Fe, and Ni) *Phys. Rev. B* **46** 5425–33
- [48] Chang A G, Lan L-W, Chan Y-J, Kuo C-N, Chen T, Huang C-H, Chuang T-H, Wei D-H, Lue C-S and Kuo C-C 2022 Trigonal distortion in zigzag-antiferromagnet iron phosphorus trisulfide *Phys. Rev. B* **106** 125412
- [49] Gong C, Li L, Li Z, Ji H, Stern A, Xia Y, Cao T, Bao W, Wang C, Wang Y, Qiu Z Q, Cava R J, Louie S G, Xia J and Zhang X 2017 Discovery of intrinsic ferromagnetism in two-dimensional van der Waals crystals *Nature* **546** 265–9
- [50] Marchiori E, Ceccarelli L, Rossi N, Lorenzelli L, Degen L C and Poggio M 2021 Nanoscale magnetic field imaging for 2D materials *Nature Reviews Physics* **4** 49-60

- [51] Chittari B L, Park Y, Lee D, Han M, MacDonald A H, Hwang E and Jung J 2016 Electronic and magnetic properties of single-layer MPX_3 metal phosphorous trichalcogenides *Phys. Rev. B* **94** 184428
- [52] Li X, Wu X and Yang J 2014 Half-Metallicity in $MnPSe_3$ Exfoliated Nanosheet with Carrier Doping *J. Am. Chem. Soc.* **136** 11065–9
- [53] Brec R, Schleich D M, Ouvrard G, Louisy A and Rouxel J 1979 Physical properties of lithium intercalation compounds of the layered transition-metal chalcogenophosphites *Inorg. Chem.* **18** 1814–8
- [54] Bhowmick A, Ganguli S and Bhattacharya M 1994 Amine intercalation in $FePS_3$: A Fe 57 Mössbauer study *Phys. Rev. B* **49** 5549–53
- [55] Somoano R B, Hadek V and Rembaum A 1973 Alkali metal intercalates of molybdenum disulfide *J. Chem. Phys.* **58** 697–701
- [56] Dresselhaus M S and Dresselhaus G 2002 Intercalation compounds of graphite *Adv. Phys.* **51** 1–186
- [57] Di Salvo F J, Hull Jr G W, Schwartz L H, Voorhoeve J M and Waszczak J V 1973 Metal intercalation compounds of TaS_2 : preparation and properties *J. Chem. Phys.* **59** 1922–9
- [58] Zhao J, Zou X, Zhu Y and Wang C 2016 Electrochemical Intercalation of Potassium into Graphite Advanced Functional Materials *Adv. Funct. Mater.* **26** 8103-8110
- [59] Stark M S, Kuntz K L, Martens S J and Warren S C 2019 Intercalation of Layered Materials from Bulk to 2D *Adv. Mater.* **31** 1808213

- [60] Rajapakse M, Karki B, Abu U O, Pishgar S, Musa M R K, Riyadh S M S, Yu M, Sumanasekera G and Jasinski J B 2021 Intercalation as a versatile tool for fabrication, property tuning, and phase transitions in 2D materials *Npj 2D Mater. Appl.* **5** 1–21
- [61] Li J, Liu W, Zhang X, Ma Y, Wei Y, Fu Z, Li J and Yan Y 2021 Heat treatment effects in oxygen-doped β -Li₃PS₄ solid electrolyte prepared by wet chemistry method *J. Solid State Electrochem.* **25** 1259–69
- [62] Kurosawa K, Saito S and Yamaguchi Y 1983 Neutron Diffraction Study on MnPS₃ and FePS₃ *Journal of the Physical Society of Japan* **52** 3919-3926
- [63] Lançon D, Ewings R A, Guidi T, Formisano F and Wildes A R 2018 Magnetic exchange parameters and anisotropy of the quasi-two-dimensional antiferromagnet NiPS₃ *Phys. Rev. B* **98** 134414
- [64] Calder S, Haglund A V, Kolesnikov A I and Mandrus D 2021 Magnetic exchange interactions in the van der Waals layered antiferromagnet MnPSe₃ *Phys. Rev. B* **103** 024414
- [65] Wildes A R, Stewart J R, Le M D, Ewings R A, Rule K C, Deng G and Anand K 2022 Magnetic dynamics of NiPS₃ *Phys. Rev. B* **106** 174422
- [66] Mauger A 1977 Indirect exchange in europium chalcogenides *Phys. Status Solidi B* **84** 761–71

Figures

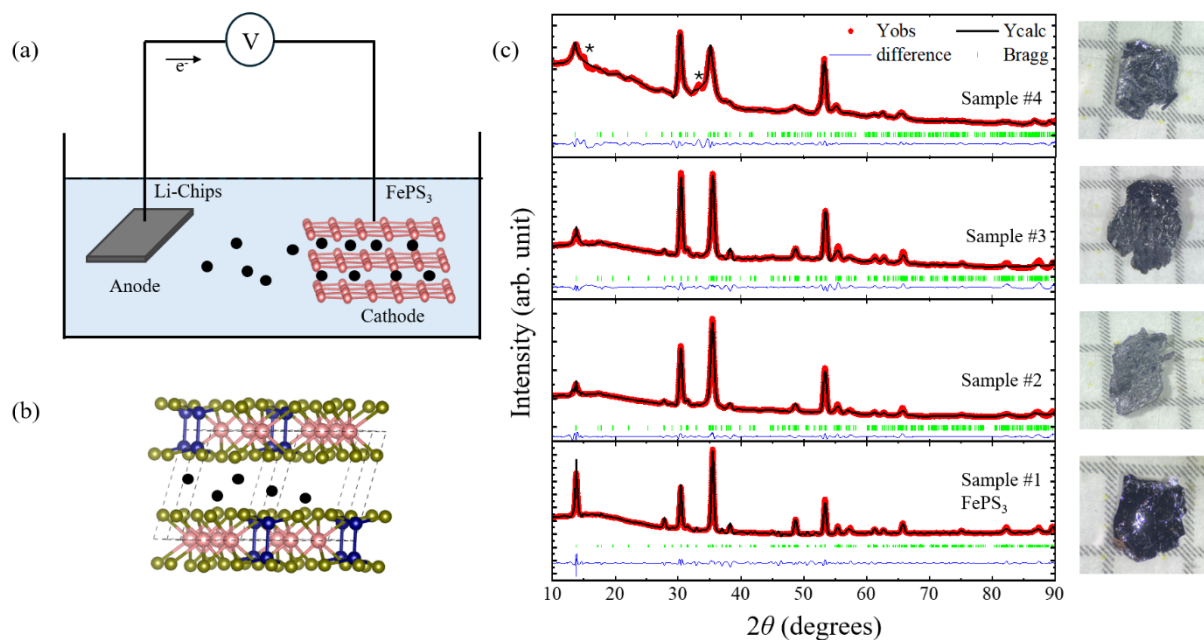


FIG. 1. (a) Conceptual schematic of the electrochemical intercalation. The intercalation was performed using a battery setup, but the concept is the same. (b) Schematic of the Li intercalation into the vdW gap of FePS₃. (c) Powder x-ray diffraction patterns and Rietveld refinement for crystal structures of pristine FePS₃ (sample #1) and various Li-intercalated (samples #2 to #4) FePS₃. Images of FePS₃ and intercalated crystals are shown in the right panel.

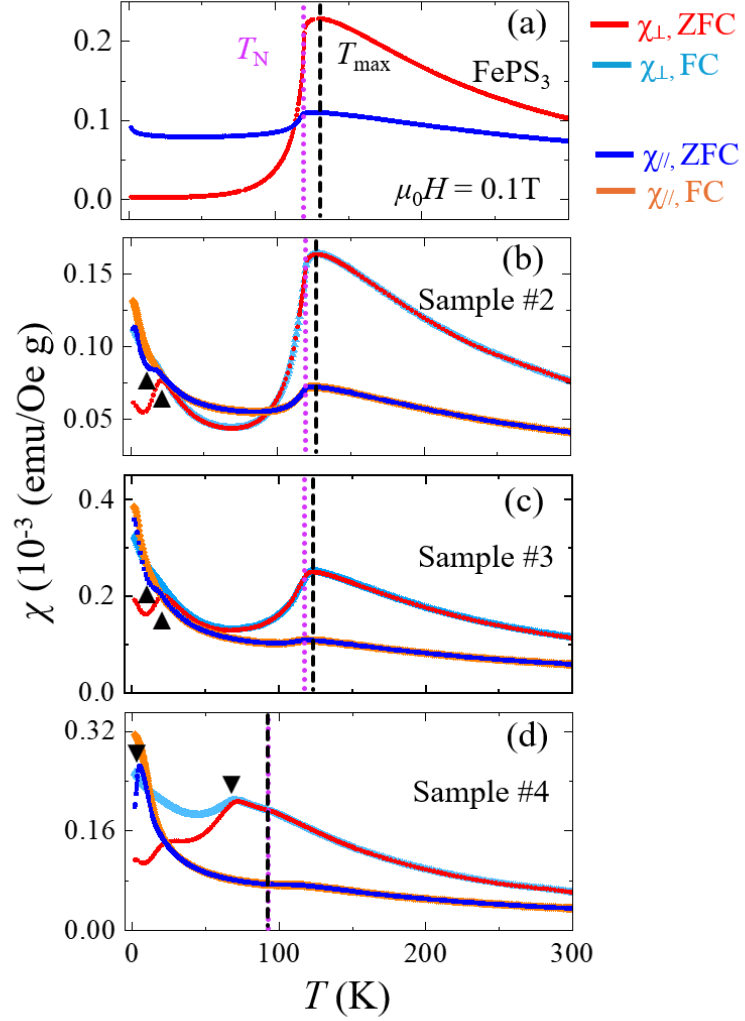


FIG. 2. Temperature dependence of out-of-plane (χ_{\perp}) and in-plane (χ_{\parallel}) susceptibilities (χ) for (a) the pristine FePS₃ (samples #1) and (b-d) Li-intercalated FePS₃ (samples #2-4). Both ZFC and FC susceptibilities are shown in intercalated samples. For the pristine FePS₃ in (a), only ZFC data are shown because its ZFC and FC data overlap. The vertical pink dotted lines and the black dashed lines denote T_N and T_{\max} , respectively. The black triangles denote T_{irr} , below which irreversibility is seen.

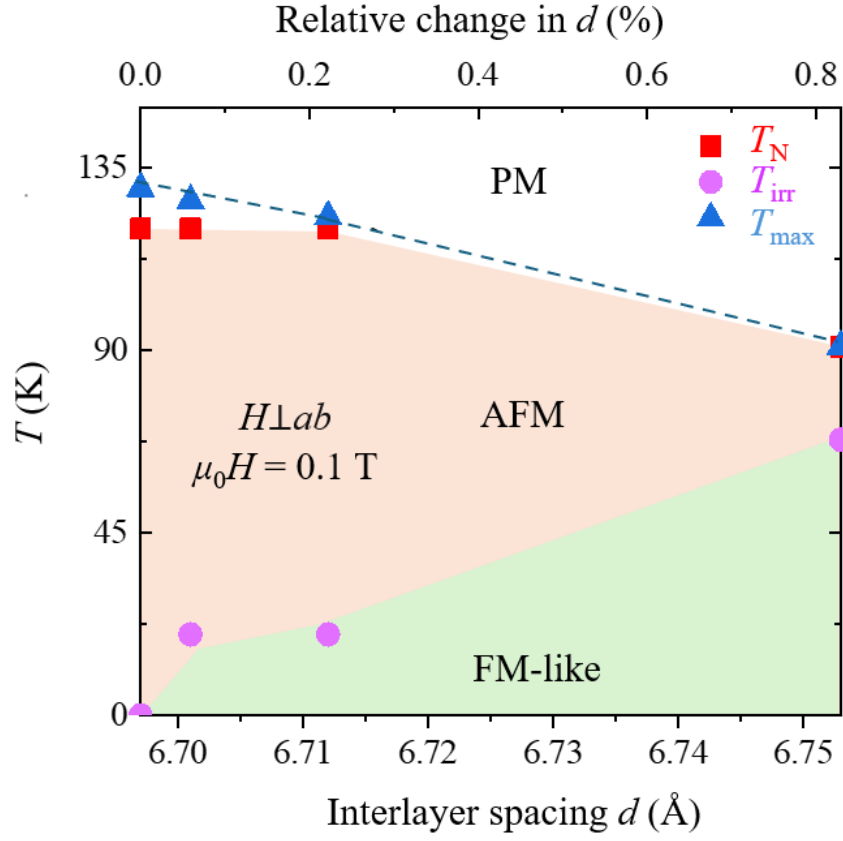


FIG. 3. Magnetic phase diagram for Li-intercalated FePS₃, showing the evolution of magnetic phases with temperature and interlayer spacing d . The phase boundaries are determined based on the out-of-plane susceptibility (χ') measured under 0.1 T magnetic field shown in Fig. 2.

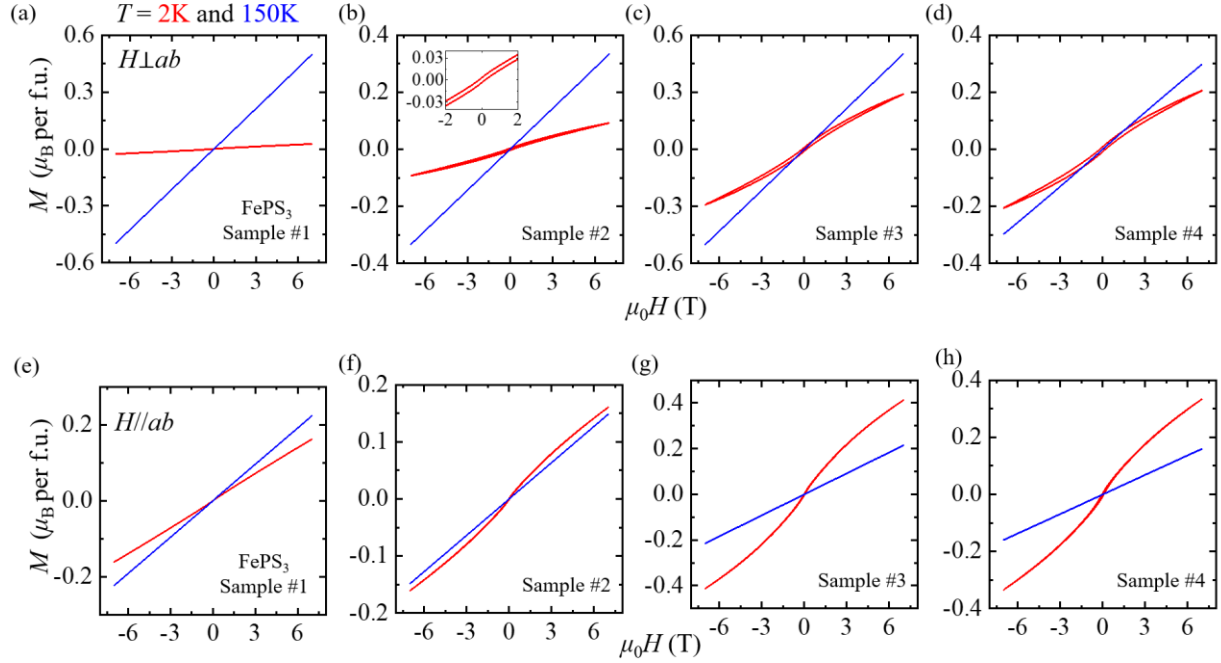


FIG. 4. Field-dependence of magnetization of the pristine (sample #1) and Li-intercalated (samples #2 to #4) FePS₃ at $T = 2$ K (red lines) and 150 K (blue lines), measured with out-of-plane ($H \perp ab$, panels a-d) and in-plane ($H // ab$, panels e-h) magnetic fields. Inset in (b) shows the low field hysteresis loop.

Tables

Table 1. Lattice parameters a , b , and c obtained from Rietveld refinement for the pristine and Li-intercalated FePS₃.

Sample	a	b	c
#1 (FePS₃)	5.94353	10.29546	6.69756
#2	5.93050	10.29169	6.70115
#3	5.95282	10.27902	6.71267
#4	5.95840	10.31935	6.75311
#5	5.94500	10.30390	7.35000

Table 2. Relative changes of magnetic ordering temperatures and inter-layer distances d in FePS₃, MnPS₃, and NiPS₃ up on intercalation.

Host materials	Relative change in d	Type of intercalation	Relative change in ordering temperature	Reference
FePS₃	54.7%	EMIM, electrochemical	-35%	43
FePS₃	47.3%	Li, liquid ammonia	Not reported	38
FePS₃	0.8%	Li, electrochemical	-24.17%	This work
MnPS₃[*]	162.6%	Amino acid, ion exchange reaction	-35.90%	40
MnPS₃[#]	91.31%	Pyridine, liquid	-23.07%	36
NiPS₃	55.72%	EMIM, electrochemical	-2.02%	43
NiPS₃	0.357%	Li, electrochemical	-1.28%	37

*Ferrimagnetism

#Weak ferromagnetism but show negative Weiss temperature